sciendo

Polish Journal of Chemical Technology, 24, 3, 19—28, 10.2478/pjct-2022-0018

Adsorption of CO_2 by surface modified coal-based activated carbons: kinetic and thermodynamic analysis

Liu Xinzhe, Zhang Mingyang*, Chen Juan, Hu Zhengyu, Xian Shuaifei, Tang Mingxuan, Zhang Chenchen

[1]*School of Thermal Engineering, Shandong Jianzhu University, Jinan 250101, Shandong, China*
**Corresponding author: e-mail: zhangmingyang18@sdjzu.edu.cn*

The effects of different surface modifiers on the CO_2 adsorption capacity of coal-based activated carbons were studied, and the diffusion behavior, adsorption kinetics and thermodynamic parameters of CO_2 in activated carbons were analyzed. The results show that compared with ethylene glycol, 1,2-propylenediamine and zinc chloride, potassium hydroxide and sodium hydroxide can greatly improve CO_2 adsorption capacity. The adsorption rate is faster, and the adsorption capacity is larger, with the maximum CO_2 adsorption capacity being 33.54 mL/g. Fick's law can well describe the diffusion behavior of CO_2 in activated carbon. The addition of a surface modifier can increase the diffusion coefficient. The diffusion of CO_2 in activated carbon falls into the category of crystal diffusion. The adsorption kinetics of CO_2 before and after surface modification follow the Bangham equation. During the adsorption process, $\delta H < 0$, $\delta G < 0$, $\delta S < 0$. Surface modification can reduce adsorption heat and promote adsorption, and the adsorption process is dominated by physisorption.

Keywords: Surface modification; CO_2 adsorption capacity; adsorption kinetics; thermodynamic parameters.

INTRODUCTION

Melting snow and glaciers contribute to continuous flow of water into the ocean. Since the start of the 20th century, the sea level has risen at a rate of 1.5–2 mm per year[1]. In the past 100 years, the global average temperature has increased by 0.74 °C, making it about 1.1 °C higher than in the pre-industrial period[2]. Global warming is mainly caused by the massive emissions of anthropogenic greenhouse gases such as CO_2, CH_4, and N_2O, of which the contribution rate of CO_2 is as high as 76%[3]. According to the data released by the Hawaii-based Mauna Loa Observatory in May 2020, CO_2 concentration hit a new high of 415.26 mg/L, the highest so far in human history[4]. Therefore, it is imperative to control the growing CO_2 concentration and reduce the rising global temperature.

In response to the multiple problems caused by CO_2, the 4th International Conference on Greenhouse Gas Control Technology held in 1998 proposed for the first time the use of separation, capture, and transportation, among other methods, to store CO_2[5]. Up to now, CO_2 capture and storage technology (carbon capture and storage, CCS) has become the most effective way to reduce CO_2 emissions in the short term. China's efforts to reduce carbon footprint are subject to economic and technological restraints. To achieve effective CO_2 emission reduction, we must start with CCS by employing existing CO_2 capture facilities[6]. At the core of CCS is CO_2 capture. So far, many CO_2 capture technologies have been developed such as absorption method, membrane separation method, and adsorption method, etc. The absorption method achieves CO_2 separation by taking advantage of the physical solubility of physical adsorbents or the chemical reaction of chemical absorbents. It features simple process flow and mature technology. However, physical absorption entails high operating costs, while chemical absorption causes severe corrosion to facilities[7]. Membrane separation method separates gas mixture by making use of selective permeability of composite membranes. A variety of driving forces are generated on both sides of the composite membrane to separate or enrich the gas. Permeability and separation coefficient are key indicators of the functionality of composite membranes. Some membranes are not resistant to high temperature or corrosion. Membrane separation method suffers from the disadvantages of huge energy consumption, heavy investment, and immature industrial application[8]. The adsorption method mainly uses solid adsorbents, which can be regenerated by changing temperature and pressure conditions[9]. Adsorption via changing temperature is called temperature swing adsorption[10], while adsorption via changing pressure is called pressure swing adsorption[11]. Pressure swing adsorption using solid adsorbents has become the most widely used CO_2 capture technology. It has the advantages of good stability, adjustable pore size and less corrosiveness. The use of CO_2 as adsorbent is due to the global problems caused by the greenhouse effect, and is in line with the hot spot in China and the world, namely carbon neutralization.

Commonly used solid adsorbents include fibers[12], ceramic materials and metal oxides[13], carbonaceous adsorbents[14], molecular sieves[15], etc. Among those solid adsorbents, activated carbon[16] is widely used in industrial fields for adsorption separation, purification and catalysis due to its developed pore structure, large specific surface area, excellent adsorption performance and stable physical and chemical properties. In this study, surface modification of activated carbon was carried out, CO_2 adsorption capacity of activated carbons surface-modified with the optimum concentration was identified, and the adsorption rate was analyzed. Zinc chloride, potassium hydroxide and sodium hydroxide are common chemical reagents for surface modification. Comparing with the common surface modification reagents, the use of ethylene glycol and 1, 2-propylenediamine for surface modification is to explore the modification effect of these two chemical reagents on coal-based activated carbons. The adsorption process and adsorption mechanism of activated carbons before and after surface modification were discussed using the diffusion coefficient, kinetic models and thermodynamic parameters.

This work takes CO_2 as adsorbent and activated carbons as adsorbent. The purpose of this study lies in the application of five chemical reagents on the surface of coal-based activated carbons and carbon dioxide adsorption. Moreover, the advantages and disadvantages of surface modification by chemical reagents are compared. The mechanism of carbon dioxide adsorption was discussed based on the adsorption kinetic model and thermodynamic parameters.

EXPERIMENT

Materials

CO_2 gas (purity ≥ 99.9%, Jinan Deyang Special Gas Co., Ltd.); iodine (analytically pure, Shanghai Macklin Biochemical Technology Co., Ltd.); activated carbon (Tianjin Beichen Founder Reagent Factory); ethylene glycol (analytically pure, Shanghai Macklin Biochemical Technology Co., Ltd.); 1,2-propylenediamine (analytically pure, Shanghai Macklin Biochemical Technology Co., Ltd.); zinc chloride (analytically pure, Shanghai Macklin Biochemical Technology Co., Ltd.); potassium hydroxide (analytically pure, Shanghai Macklin Biochemical Technology Co., Ltd.); sodium hydroxide (analytically pure, Shanghai Macklin Biochemical Technology Co., Ltd.); laboratory-made deionized water.

Determination of CO_2 adsorption capacity of activated carbon

Gravimetric method was chosen to conduct CO_2 adsorption capacity measurement, using a NETZSCH STA409PC thermogravimetric analyzer. Before the test, the samples were dried at 300 °C for 60 min to remove the moisture and residual gas in the activated carbon. Then the activated carbon samples were cooled to 25 °C for the measurement of the CO_2 adsorption capacity of the chestnut shell-based carbon material. The CO_2 flow rate was 60 mL/ min. The formula used to calculate CO_2 adsorption amount q_t ($mL \cdot g^{-1}$) is:

$$q_t = \frac{m_t - m_0}{m_0} * \frac{1}{44} * 100 \quad (1)$$

Where $m_{t\ (g)}$ is the mass of the sample at any time of adsorption, $m_{0\ (g)}$ is the mass of the sample at the initial time of adsorption.

Analytical Test Instruments

Electronic analytical balance (FA224TC, Shanghai International Scientific Instrument Co., Ltd.); electric heating blast drying oven (FCHB-C6000, Zhongyi Guoke Beijing Technology Co., Ltd.); collector-type constant temperature heating magnetic stirrer (DF-101S, Shanghai Bangxi Lichen Instruments Technology Co., Ltd.); specific surface area and pore size tester (ASAP 2020 HD88, Mike Instruments, USA); thermal analyzer (STA409PC, Agilent Technologies Co., Ltd.).

Surface modification of activated carbons

The surface modification of activated carbons is carried out as follows:

(1) Accurately weighed 1g of activated carbon was placed in a 100 mL conical flask. Then 50 mL of deionized water was added into the conical flask, which was subsequently placed in a constant temperature heating magnetic stirrer. The stirring temperature was set at 25 °C. The conical flask was taken out after 3 hours and put in an electric heating blast drying oven. The drying temperature was 120 °C. After drying for 24 h, the surface-modified activated carbon was used to adsorb CO_2. The adsorption temperature was set at 25 °C, and the adsorption pressure was 1.0 MPa. The CO_2 adsorption capacity was determined to be 10.32 mL/g. The sample number was BAC.

(2) Accurately weighed 1g of activated carbon was placed in a 100 mL conical flask. The concentration of ethylene glycol solution was 0.25 mol/L, 0.5 mol/L, 0.75 mol/L, 1.0 mol/L, 2.0 mol/L, 3.0 mol/L, 4.5 mol/L, 6.0 mol/L, respectively, and the volume was 50 mL. The samples were labeled as HA-01, HA-02, HA-03, HA-04, HA-05, HA-06, HA-07 and HA-08, respectively; the stirring temperature was set at 25 °C. After 3 hours, the conical flask was taken out and put into an electric heating blast drying oven. The drying temperature was 120 °C. After drying for 24 hours, it was used to adsorb CO_2. The adsorption temperature was 25 °C, and the adsorption pressure was 1.0 Mpa. The optimum concentration for surface modification is determined by the amount of CO_2 adsorption. The optimum concentration of ethylene glycol for surface modification was 1.0 mol/L, and the corresponding CO_2 adsorption capacity was 14.71 mL/g. The sample was labeled as HA-04.

(3) 1,2-propylenediamine, zinc chloride, potassium hydroxide and sodium hydroxide were used for surface modification, respectively, and the treatment was the same as that in step 2 for each surface modifier. The optimum concentration of 1,2-propylenediamine for surface modification was 1.0 mol/L, the corresponding CO_2 adsorption capacity was 23.88 mL/g, and the sample number was RW-04; the optimum concentration of zinc chloride for surface modification was 1.0 mol/L, the corresponding CO_2 adsorption capacity was 20.34 mL/g, and the sample was labeled as Zn-04; the optimum concentration of potassium hydroxide for surface modification was 2.0 mol/L, the corresponding CO_2 adsorption capacity was 33.52 mL/g, and the sample number was K-05; the optimum concentration of sodium hydroxide for surface modification was 0.75 mol/L, the corresponding CO_2 adsorption capacity was 32.69 mL/g, and the sample was labeled as Na-03.

Characterization of activated carbons

The apparent density of activated carbons was determined in accordance with the national standard GB/T12496.1-1999[17], and the iodine adsorption value was determined in accordance with the national standard GB/T12496.8-2015[18]. Surface pore structure parameters of activated carbons were determined with nitrogen as the adsorbate at 77K using a specific surface area and pore size analyzer (ASAP 2020 HD88, Mike Instruments, USA), and the type of nitrogen adsorption/desorption curve was determined[19]. The BET equation[20] was used to calculate the specific surface area of activated carbon, and the BJH equation[21] was employed to determine the pore volume and pore size of activated carbons. The physical parameters of the activated carbon materials are shown in Table 1.

Table 1. Physical property parameters of activated carbon materials

Activated carbon	BAC	HA-04	RW-04	Zn-04	K-05	Na-03
Apparent density/ ($g \cdot mL^{-1}$)	0.455	0.467	0.477	0.481	0.483	0.479
Particle size/(um)	75	75	75	75	75	75
Iodine adsorption value / ($mg \cdot g^{-1}$)	231	245	262	274	287	289
N_2 adsorption line type	Type Ⅱ	Type Ⅱ	Type Ⅱ	Type Ⅱ	Type Ⅱ	Type Ⅱ
Specific surface area / ($m^2 \cdot g^{-1}$)	10.366	6.974	7.323	21.083	7.539	9.907
Pore volume / ($cm^3 \cdot g^{-1}$)	0.02969	0.02411	0.02609	0.1272	0.02621	0.02539
Average pore size / (nm)	8.302	15.108	9.864	17.549	8.711	15.808
Median pore size / (nm)	27.058	24.941	23.567	42.551	20.648	18.582

EXPERIMENTAL RESULTS AND DISCUSSION

Analysis of CO_2 adsorption performance of activated carbons

The adsorption temperature was set at 25 °C, and the CO_2 flow rate was 60 mL/min. The saturation capacities of activated carbons for CO_2 adsorption were determined. Fig. 1 shows the adsorption process. It can be seen that the adsorption of CO_2 by BAC is a relatively gradual process, that is, no dramatic increase occurred at a certain time point. The adsorption reached saturation around 15 min in a gradual manner, and the adsorption amount changed little after 15 min. The surface modification of ethylene glycol not only enhances the adsorption capacity of activated carbons but also increases the adsorption efficiency. HA-04 gradually reached adsorption equilibrium around 10 minutes. Compared with ethylene glycol, 1, 2-propylenediamine can improve the adsorption efficiency greatly. During the entire adsorption process, the adsorption amount of RW-04 increased steadily, which indicates that the adsorption of RW-04 for CO_2 may involve a certain degree of chemical adsorption[22]. In this case, the adsorption was affected by the surface chemical bonds, resulting in a continuous adsorption process. Zn-0, K-05 and Na-03 exhibit similar adsorption processes. To be specific, the adsorption capacity increased rapidly within 7.5 min, adsorption basically reached saturation within 10 min, and there was no marked change after 10 min. Therefore, the adsorption of Zn-04, K-05 and Na-03 fall into the category of physical adsorption[23] and is mainly affected by the van der Waals force, that is, directional force, inductive force and dispersion force. The adsorbed CO_2 molecules were prone to desorption. Desorption and adsorption reached equilibrium within a very short time range, which means the amount of CO_2 adsorption reached saturation within a short period of time and then stabilized over time.

CO_2 diffusion coefficient

Adsorption is defined as follows: the surface of activated carbons spontaneously uses its unsaturated free valence at a certain temperature to capture the molecules in the adsorbed phase, reducing the surface Gibbs free energy of molecules by concentrating them on the phase interface. The indicators for evaluating the adsorption performance of activated carbons are adsorption capacity and adsorption speed. The adsorption capacity is measured by the amount of CO_2 adsorption, while the

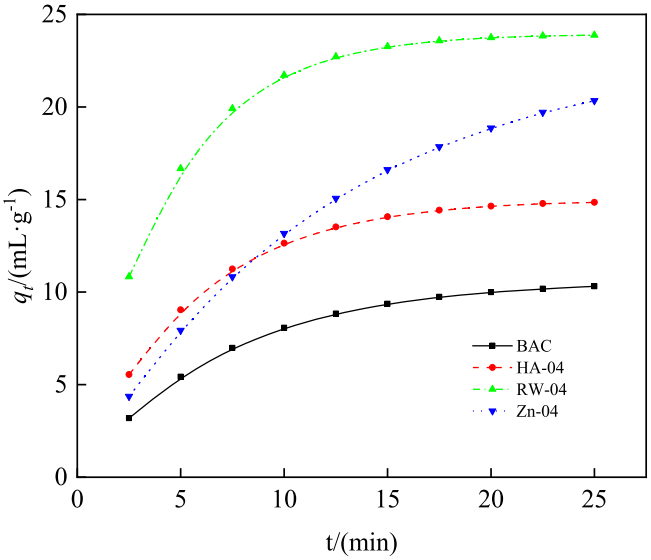

(a) BAC, HA-04, RW-04, Zn-04

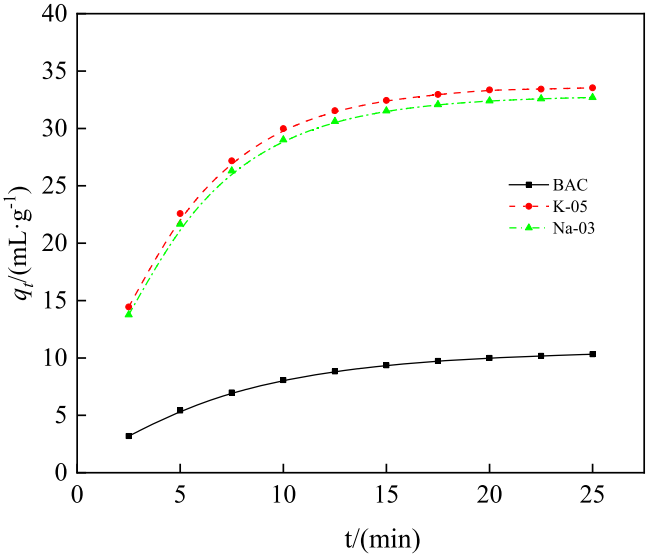

(b) BAC , K-05, Na-03

Figure 1. Saturation process of CO_2 adsorption by activated carbons

adsorption speed is determined by the amount of CO_2 adsorption per unit mass of activated carbon per unit time. The adsorption process can be divided into three stages: (1) the external diffusion stage of the particles when the adsorbate diffuses from the adsorbed phase to the surface of the adsorbent; (2) the pore diffusion stage when the adsorbate continues to diffuse to the adsorption

site through the adsorbent pores; (3) adsorption reaction stage when the adsorbate is adsorbed on the surface of adsorption sites within the pores of the adsorbent. Among the three stages, adsorption reaction is completed in a very short time; therefore, the adsorption speed is mainly determined by the speed of external diffusion and pore diffusion. The diffusion behavior of adsorbate molecules inside the adsorbent is described by Fick's second law[24]. The adsorption kinetic curve can generally be divided into fast adsorption in the initial stage of adsorption and slow adsorption in the stable adsorption stage. Due to the instability of the system in the initial stage, the kinetic equation for slow adsorption is suitable for the calculation of the diffusion coefficient.

Assuming that activated carbon consists of homogeneous particles, that the adsorbate concentration on the particle surface is constant, and that the temperature of the entire adsorption system is constant, then for the slow adsorption stage ($q_t/q_\infty>0.5$) we get:

$$\frac{q_t}{q_\infty}=1-\frac{6}{\Pi^2}\exp\left(-\frac{D\Pi^2 t}{r^2}\right) \tag{2}$$

Where q_∞ (mL · g^{-1}) is the saturated adsorption capacity, D(m^2 · s^{-1}) is the diffusion coefficient, t (min) is the adsorption time, and r(m) is the average particle radius.

Taking the natural logarithm of equation (2) gives:

$$-\ln(1-\frac{q_t}{q_\infty})=\frac{D\Pi^2}{r^2}t-\ln\frac{6}{\Pi^2} \tag{3}$$

In formula (3), the dependent variable and the independent variable are $-\ln(1-q_t/q_\infty)$ and t respectively; then the value of $D\Pi^2/r^2$ can be obtained by linear regression within the range of $q_t/q_\infty>0.5$, and the value of diffusion coefficient D can be obtained. Based on formula (3), a linear regression was performed on the change curve of CO_2 adsorption amount relative to time in Fig. 1, and the results are shown in Table 2. It can be seen that surface modification increases the diffusion coefficient. Generally, the diffusion of molecules within porous media can be classified into four categories: free diffusion (D: 10^{-5} ~ 10^{-4}), Kundsen diffusion (D: 10^{-7} ~ 10^{-6}), surface diffusion (D < 10^{-7}) and crystal diffusion (D<10^{-9}). According to Table 2, the diffusion of CO_2 within activated carbons before and after surface modification belong to crystal diffusion.

Table 2. Diffusion coefficient of CO_2 in activated carbons

Activated carbon	D/(m^2 · s^{-1})	R^2
BAC	3.963 * 10^{-10}	0.991
HA-04	4.218 * 10^{-10}	0.993
RW-04	4.878 * 10^{-10}	0.992
Zn-04	4.674 * 10^{-10}	0.994
K-05	5.689 * 10^{-10}	0.995
Na-03	5.311 * 10^{-10}	0.991

Kinetic analysis of CO_2 adsorption on activated carbons

The quasi-first-order kinetic model, the quasi-second-order kinetic model, the intra-particle diffusion model, the Elovich kinetic model and the Bangham kinetic model are the most widely used kinetic models in the investigation of adsorption kinetics. Among them, the quasi-first-order kinetic model and the Bangham model are used to clarify whether the adsorption process is physical adsorption. And, the quasi-second-order kinetic model is used to indicate whether the adsorption process is chemical adsorption, the intra-particle diffusion model is used to judge the location of physical adsorption. Moreover, the Elovich model is used to judge the reaction between adsorbent and adsorbent.

Quasi-first-order kinetic model

The quasi-first-order kinetic model[25] is based on the membrane diffusion theory, which assumes that the adsorption is subject to the diffusion stages and that the adsorption reaction rate of the adsorbate is positively proportional to the first power of the difference between the values of equilibrium adsorption capacity and the actual adsorption capacity in the system. The adsorption rate can be calculated using the Lagergren equation:

$$\frac{dq_t}{dt}=K_1(q_e-q_t) \tag{4}$$

Applying the boundary conditions t = 0 to t = t and the corresponding values q_t = 0 to q_t = q_t to equation (4) for integration, we can obtain:

$$q_t=q_e-q_e e^{-K_1 t} \tag{5}$$

Where q_t (mL · g^{-1}) is the adsorption amount of CO_2 at time t, q_e (mL · g^{-1}) is the adsorption amount of CO_2 at equilibrium, t (min) is the adsorption time, and K_1 (min^{-1}) is quasi-first-order adsorption rate constant.

The fitting parameters of CO_2 adsorption on activated carbon using the quasi-first-order kinetic model are shown in Table 3, and the curve fitting is shown in Fig.2.

Quasi-second-order kinetic model

The quasi-second-order kinetic model[26] assumes that the adsorption rate is determined by the square of the number of unoccupied adsorption vacancies on the adsorbent surface and that the adsorption process is subject to chemisorption mechanism, which involves the sharing or transfer of electrons between adsorbents and adsorbates. The equation is:

$$\frac{dq_t}{dt}=K_2(q_e-q_t)^2 \tag{6}$$

Applying the boundary conditions t = 0 to t = t and the corresponding values q_t = 0 to q_t = q_t to integrate equation (6), we get:

$$\left(\frac{t}{q_t}\right)=\frac{1}{K_2 q_e^2}+\frac{t}{q_t} \tag{7}$$

Table 3. Fitting parameters of CO_2 adsorption using the quasi-first-order kinetic model

Quasi-first-order kinetic model	BAC	HA-04	RW-04	Zn-04	K-05	Na-03
$q_{e,exp}$/ (mL • g^{-1})	10.317	14.850	23.885	20.351	33.543	32.698
$q_{e,cal}$/ (mL • g^{-1})	10.606	15.015	23.936	23.231	32.658	32.828
K_1	0.143	0.184	0.239	0.084	0.221	0.216
R^2	0.999	0.999	0.999	0.999	0.999	0.999

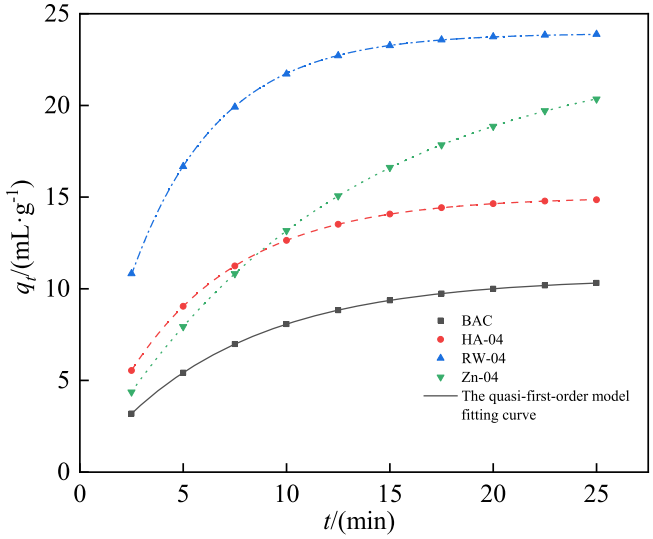

(a) BAC, HA-04, RW-04, Zn-04

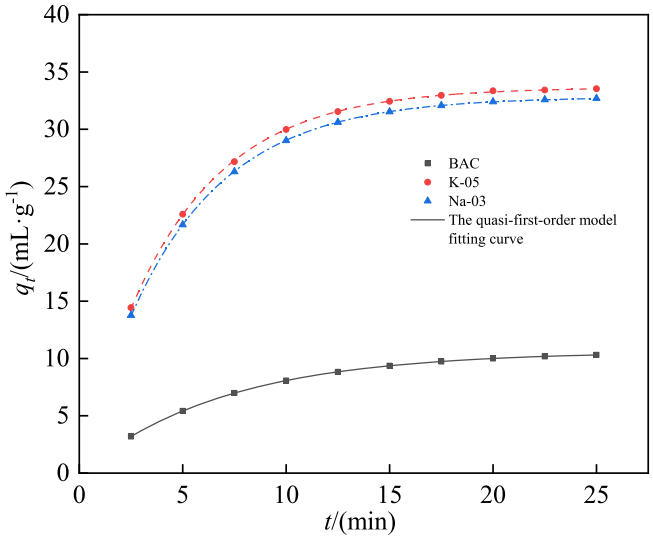

(b) BAC, K-05, Na-03

Figure 2. Curve fitting of CO_2 adsorption by activated carbons using the quasi-first-order kinetic model

Rearranging formula (7), we get:

$$q_t = \frac{K_2 q_e^2 t}{1 + K_2 q_e t} \tag{8}$$

Where q_t (mL · g^{-1}) is the CO_2 adsorption amount at time t, q_e (mL · g^{-1}) is the CO_2 adsorption amount when the adsorption reaches equilibrium, t (min) is the adsorption time, and K_2 (mL · g^{-1} · min^{-1}) is quasi-second order adsorption rate constant. The initial adsorption rate can be calculated using the quasi-second-order adsorption rate constant, and the calculation formula is as follows:

$$h = K_2 q_e^2 \tag{9}$$

Table 4 shows the fitting parameters of CO_2 adsorption by activated carbon using the quasi-second-order kinetic model, and the curve fitting is shown in Fig. 3.

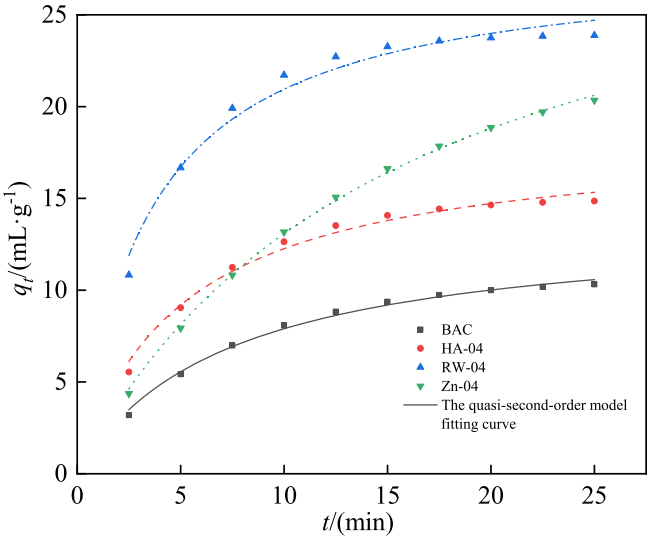

(a) BAC, HA-04, RW-04, Zn-04

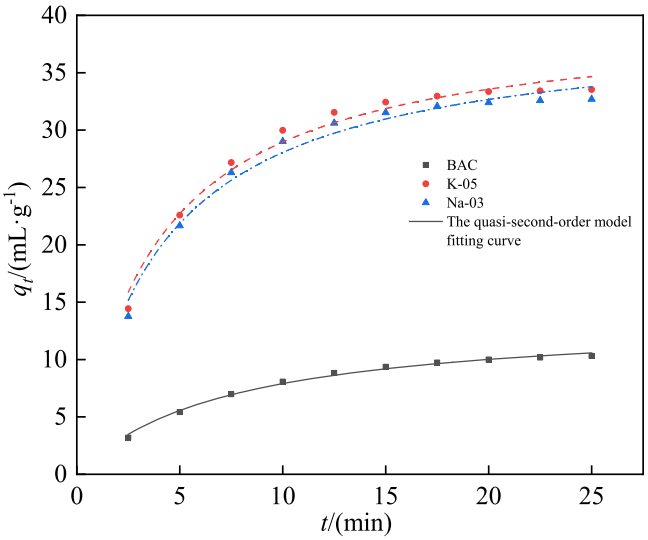

(b) BAC, K-05, Na-03

Figure 3. Curve fitting of CO_2 adsorption by activated carbons using the quasi-second-order model

Intra-particle diffusion model

The intra-particle diffusion model[27] assumes the following conditions: (1) the diffusion resistance of the adsorption contact surface is negligible or the diffusion resistance only works for a short time in the initial stage of adsorption; (2) the diffusion direction is random, and the adsorbate concentration is independent of the particle position; (3) the internal diffusion coefficient is constant and does not change with the adsorption time

Table 4. Fitting parameters of CO_2 adsorption using the quasi-second-order kinetic model

Quasi-Second-Order Dynamics Model	BAC	HA-04	RW-04	Zn-04	K-05	Na-03
$q_{e,exp}$/ (mL • g^{-1})	10.317	14.850	23.885	20.351	33.533	32.698
$q_{e,cal}$/ (mL • g^{-1})	13.6537	18.408	28.023	33.482	39.925	39.123
K_2	0.011	0.011	0.011	0.001	0.006	0.006
h/(mL • min^{-1})	2.052	3.727	8.638	1.121	9.564	9.183
R^2	0.994	0.987	0.977	0.998	0.981	0.982

and adsorption position. Therefore, the intraparticle diffusion model is a kinetic model that studies the rate limit of adsorption. Its calculation formula is:

$$q_t = K_{dif} t^{1/2} + C \quad (10)$$

Where q_t (mL · g^{-1}) is the amount of CO_2 adsorption at time t, C is the intercept constant, t (min) is the adsorption time, and K_{dif}(mL · g^{-1} · min$^{-1/2}$.) is the intraparticle diffusion rate constant

The parameters related to the fitting of CO_2 adsorption by activated carbon using the intra-particle diffusion model are shown in Table 5, and the curve fitting is shown in Fig.4.

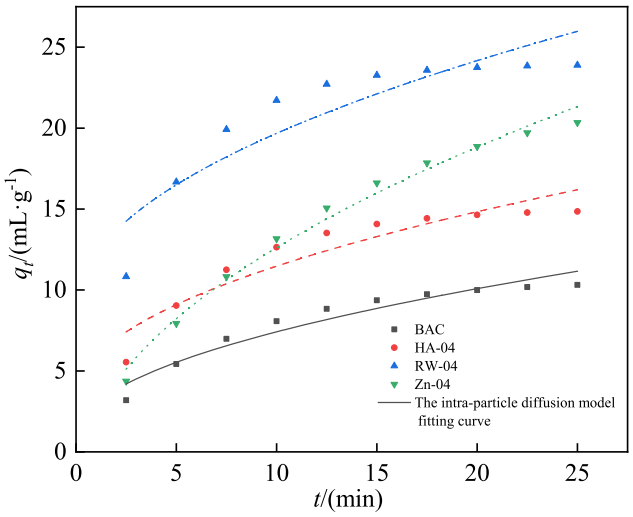

(a) BAC, HA-04, RW-04, Zn-04

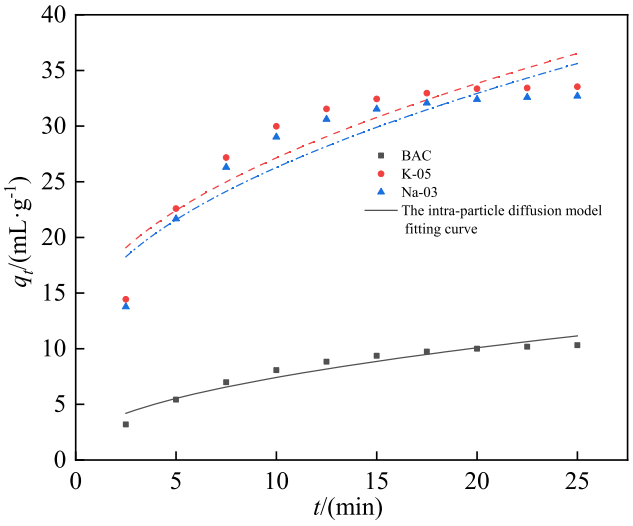

(b) BAC, K-05, Na-03

Figure 4. The intra-particle diffusion model fitting curve of CO_2 adsorption by activated carbons

Elovich kinetic model

The Elovich kinetic model[28] is used to analyze the adsorption behavior of adsorbates on the surface of heterogeneous solid adsorbents. Although this model does not make any explicit assumptions for the interaction mechanism between adsorbates and adsorbents, it can describe the kinetics of chemical adsorption. The Elovich kinetic model can reveal the irregular shape of data ignored by other kinetic models and is suitable for adsorption reaction processes with large activation energy. It can be expressed as:

$$\frac{dq_t}{dt} = \alpha \exp(-\beta q_t) \quad (11)$$

Assuming αβ>>t for formula (11), using boundary conditions t=0, t=t, and its corresponding values q_t=0, q_t=q_t, the above formula can be rearranged as:

$$q_t = \frac{1}{\beta}\ln(\alpha\beta) + \frac{1}{\beta}\ln(t) \quad (12)$$

Where q_t (mL · g^{-1}) is the amount of CO_2 adsorption at time t, t (min) is the adsorption time, α(mL · g^{-1} · min^{-1}) is the initial rate constant, and β (g · mL^{-1}) is the desorption rate constant.

The fitting parameters of CO_2 adsorption by activated carbon using the Elovich kinetic model are shown in Table 6, and the curve fitting is shown in Fig. 5.

Bangham kinetic model

The Bangham formula[29] can be written in the following form:

$$\frac{dq_t}{dt} = K_B (q_e - q_t)^z \quad (13)$$

Using the boundary conditions t = 0, t = t and its corresponding values q_t = 0, q_t = q_t to integrate the formula, we get:

$$\ln\left(\frac{q_e}{q_e - q_t}\right) = K_B t^Z \quad (14)$$

Equation (14) can be rearranged into the following linear form:

$$q_t = q_e - q_e e^{-K_B t z} \quad (15)$$

Where qt (mL · g^{-1}) is the CO_2 adsorption amount at time t, q_e (mL · g^{-1}) is the CO_2 adsorption amount when the adsorption reaches equilibrium, and t (min) is the adsorption time, and K_B and Z are constants.

Table 7 shows the fitting parameters of CO_2 adsorption by activated carbon using the Bangham kinetic model, and the curve fitting is shown in Fig. 6.

The quasi-first-order kinetic model, the quasi-second--order kinetic model, the intra-particle diffusion model,

Table 5. Fitting parameters of CO_2 adsorption using the intra-particle diffusion model

Intraparticle diffusion model	BAC	HA-04	RW-04	Zn-04	K-05	Na-03
K_{dif}	2.035	2.569	3.432	4.745	5.104	5.078
C	0.982	3.346	8.824	–2.385	11.009	10.225
R^2	0.934	0.883	0.818	0.987	0.839	0.846

Table 6. Fitting parameters of CO_2 adsorption using the Elovich kinetic model

Elovich kinetic model	BAC	HA-04	RW-04	Zn-04	K-05	Na-03
α	3.678	7.565	21.296	4.701	24.889	22.749
β	0.313	0.243	0.179	0.138	0.121	0.122
R^2	0.989	0.966	0.927	0.993	0.941	0.944

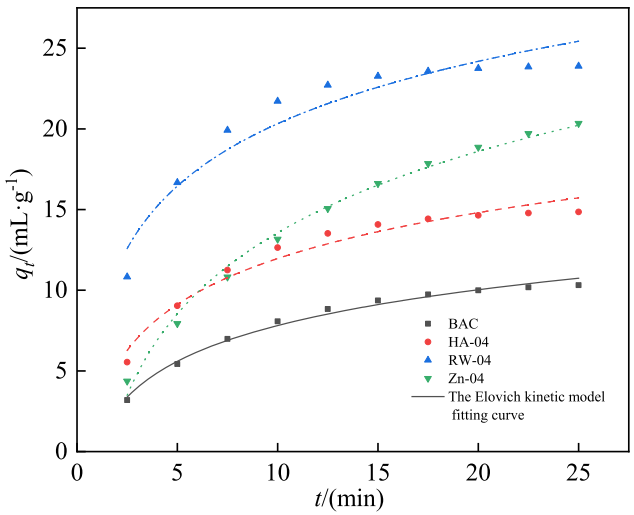

(a) BAC, HA-04, RW-04, Zn-04

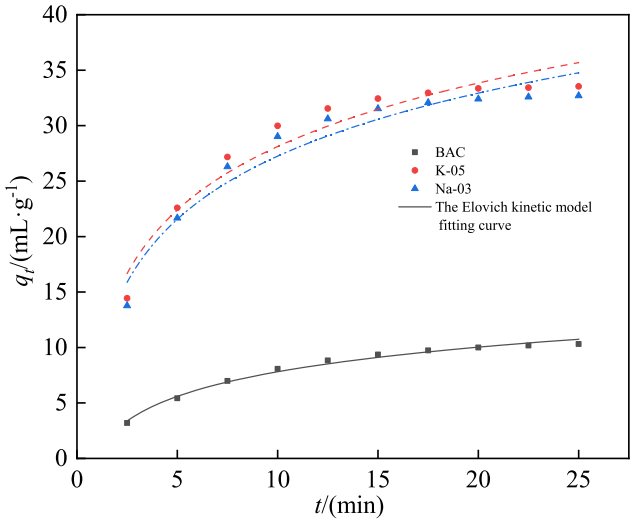

(b) BAC, K-05, Na-03

Figure 5. Curve fitting of CO_2 adsorption by activated carbons using the Elovich kinetic model

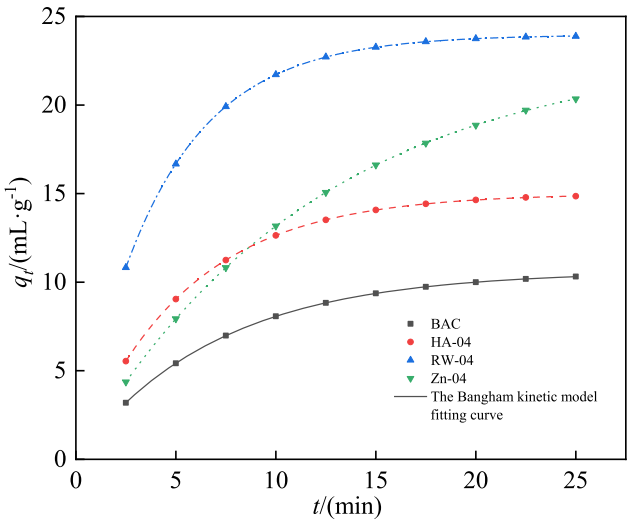

(a) BAC, HA-04, RW-04, Zn-04

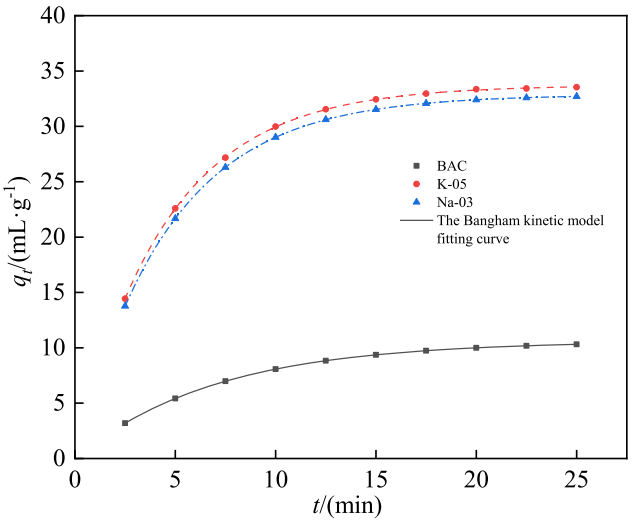

(b) BAC, K-05, Na-03

Figure 6. Curve fitting of CO_2 adsorption by activated carbons using the Bangham kinetic model

the Elovich kinetic model and the Bangham kinetic model were used to investigate the variation of adsorption capacity along with time. The fitting adaptability of these five kinetic models can be evaluated by fitting correlation coefficient R^2. With respect to the best fit (R^2), the order was: the Bangham kinetic model > the quasi-first-order kinetic model > the Elovich kinetic model > the quasi-second-order kinetic model > the intra-particle diffusion model. From fitting correlation coefficient R^2, it can be seen that the experimental data were best described by the Bangham model, which reveals that there is a linear relationship between the carbon dioxide adsorption capacity and the adsorption pressure. Therefore, the linear relationship indicated that the adsorption process is dominated by physisorption. Moreover, the quasi-second-order kinetic model is not suitable for describing the adsorption process. The result indicated that the CO_2 adsorption is not built on the basis of chemical adsorption.

Thermodynamic analysis of activated carbons adsorption of CO_2

Isosteric heat analysis

The heat of adsorption refers to the thermal effect produced in the adsorption process. During adsorption, the gas molecules move onto the surface of the adsorbent and their molecular motion is greatly reduced, resulting

Table 7. Fitting parameters of CO_2 adsorption using the Bangham kinetic model

Bangham kinetic model	BAC	HA-04	RW-04	Zn-04	K-05	Na-03
$q_{e,exp}$/(mL • g^{-1})	10.317	14.850	23.885	20.351	33.543	32.698
$q_{e,cal}$/(mL • g^{-1})	10.069	15.011	23.966	21.164	33.719	32.866
K_B	0.143	0.184	0.243	0.833	0.226	0.219
Z	0.999	1.001	0.988	1.004	0.986	0.991
R^2	1	1	1	1	0.999	1

in heat release. Isosteric heat of adsorption[30] refers to the enthalpy change of adsorbing 1 mol of gas when the adsorption temperature, adsorption pressure, and adsorbent surface area are constant. It can reflect in an indirect manner the adsorption strength, the inhomogeneity of the adsorbent surface, and the type of adsorption. Isosteric heat of adsorption is usually calculated using the Glausius-Clapeyron equation:

$$\frac{1}{P}\frac{d_P}{d_T} = \frac{q_{est}}{RT^2} \tag{16}$$

Rewriting and integrating give:

$$\ln P = -\frac{q_{est}}{RT} + C \tag{17}$$

Where q_{est} (KJ mol^{-1}) is the isosteric heat of adsorption (a value equal to the enthalpy change ΔH during the adsorption process), R (J · mol^{-1} · K^{-1}) is the ideal gas constant, T (K) is the adsorption temperature, P (Pa) is the adsorption equilibrium pressure, and C is constant. The isosteric adsorption heat q_{est} for CO_2 adsorption by activated carbon is shown in Table 8.

It can be seen from Table 8 that the chemical reagents can reduce the adsorption heat during the adsorption process, which indicates that the chemical reagents are helpful carbon dioxide molecules entering the interior of coal-based activated carbon more easily. Based on the specific numerical value of isosteric heat of adsorption, the equal heat of adsorption is less than 40 KJ/mol. It indicated that the adsorption process is physical adsorption. And, potassium hydroxide shows the best modification effect.

Adsorption free energy analysis

Free energy refers to the part of internal energy that is reduced within the system that can be converted into work during a thermodynamic process. The Gibbs free energy in the adsorption process[31] refers to the increase of the free energy of the system with the increase of the unit area of the adsorbent under constant temperature and pressure. The adsorption free energy ΔG can be used to determine the adsorption mechanism, and its formula is:

$$\Delta G = -RT \ln K_d \tag{18}$$

Where ΔG (KJ · mol^{-1}) is the Gibbs free energy change of adsorption, R (J · mol^{-1} · K^{-1}) is the ideal gas constant, T (K) is the adsorption temperature, and K_d is the adsorption thermodynamics equilibrium constant. In our study, K_d is calculated using the fitting parameters of the Freundlich equation, that is, $K_d = K_{fn}$. The Freundlich equation is:

$$q_e = K_{fn} P^{\frac{1}{n_F}} \tag{19}$$

Table 8 shows the adsorption thermodynamic equilibrium constant K_{fn} and adsorption free energy ΔG of activated carbon for CO_2 adsorption.

In Table 8, it can be judged that the addition of chemical reagents lead to the increase of the adsorption free energy of carbon dioxide during the adsorption process. Generally, the adsorption free energy of chemical adsorption than of physical adsorption, which indicates that the addition of chemical reagents lead to the change of structure of coal-based activated carbon. Consequently, the capacity of chemical adsorption of coal-based activated carbon increases. However, physical adsorption plays a dominant role.

Adsorption entropy analysis

Entropy is a measure of the degree of rearrangement or disorder of a thermodynamic system. Adsorption entropy ΔS[32] refers to the change in the entropy of the adsorbate during the adsorption process. Reflecting the interaction between the adsorbate and the adsorbent, adsorption entropy ΔS can be used to understand the movement or arrangement of the adsorbate molecules on the surface of the adsorbent. The adsorption entropy ΔS can be calculated using the Gibbs-Helmholtz equation:

$$\Delta S = \frac{\Delta H - \Delta G}{T} \tag{20}$$

Where ΔS (J · mol^{-1} · K^{-1}) is the adsorption entropy, ΔH (KJ · mol^{-1}) is the adsorption enthalpy change, ΔG (KJ · mol^{-1}) is the Gibbs free energy change of adsorption, and T (K) is the adsorption temperature. The adsorption entropy ΔS of activated carbon for CO_2 adsorption is shown in Table 8.

From Table 8, it can be concluded that the modification of chemical reagents leads to the reduction of adsorption entropy in the process of carbon dioxide adsorption, which indicated that the addition of chemical reagents is beneficial to promoting the carbon dioxide molecules into the coal-based activated carbon. The chaos degree of carbon dioxide molecules in coal-based activated carbons was reduced. So, more carbon dioxide molecules can be stored in coal-based activated carbons.

Table 8. Thermodynamic parameters of CO_2 adsorption by activated carbons

Thermodynamic parameters	BAC	HA-04	RW-04	Zn-04	K-05	Na-03
q_{est}/(KJ • mol^{-1})	-34.221	-29.257	-18.154	-23.569	-13.784	-14.412
K_{fn}	10.422	15.263	24.508	21.004	34.641	33.373
ΔG/(KJ • mol^{-1})	-5.087	-6.752	-7.879	-7.543	-6.499	-6.611
ΔS/(J • mol^{-1} • K^{-1})	-97.716	-75.482	-34.463	-53.751	-24.434	-26.165

Table 9. Comparison with CO_2 adsorbents from other studies

CO_2 adsorbents	CO_2 adsorption capacity	Modified chemical reagent	Citing paper
Activated carbon	33.54 mL/g	KOH	This paper
Sawdust	4.25 mmol/g	KOH	Jin et al.[32]
Silica	164 mg/g	Non-modified reagent	Jiao et al.[33]
Nitride/HKUST-1 Hybrid Materials	163 cm^3/g	Non-modified reagent	Jia et al.[34]
Zeolite	1.48 mmol/g	Non-modified reagent	Pham et al.[35]
Activated carbon fibers	250 mg/g	KOH	Lee et al.[36]

Comparison with CO_2 adsorbents from other studies

According to the comparison of CO_2 adsorption capacity in Table 9, it can be seen that surface modification of activated carbon by KOH in this paper can obtain a large CO_2 adsorption capacity, which indicates that modification of activated carbon by KOH can effectively promote the adsorption of CO_2 by activated carbon.

CONCLUSION

(1) Fick's law can well describe the diffusion behavior of CO_2 in activated carbons before and after surface modification. The diffusion of CO_2 in activated carbons belongs to crystal diffusion. Surface modification can increase the diffusion coefficient, which means that surface modification will make it easier for CO_2 molecules to enter the activated carbons.

(2) The Bangham kinetic model has the highest fitting degree. The correlation coefficient R^2 obtained through Bangham kinetic model fitting was higher than 0.99, and the expected value q_e calculated from the Bangham kinetic model was fairly close to the experimental value of q_e. Those results show that the Bangham kinetic model can describe the adsorption kinetics of CO_2 on activated carbons very well.

(3) From the adsorption curve of activated carbons before and after surface modification, it can be concluded that the adsorption amount increased rapidly in the initial stage of adsorption, which indicates that the adsorption of CO_2 by activated carbons mainly occurs in the monolayer outer surface and that surface modification increases the adsorption rate of activated carbons in the initial stage.

(4) The isosteric adsorption heat q_{est} was less than 40KJ · mol^{-1}, which indicates that the adsorption of CO_2 by activated carbons is physical adsorption and that the adsorption force in play is van der Waals force. Surface modification reduced the isosteric adsorption heat q_{est}, resulting in easier adsorption. The adsorption free energy ΔG increased, which indicates that the kinetic energy of the adsorbed gas increased. The adsorption entropy ΔS decreased, which indicates that the surface modification reduces the degree of freedom of the adsorbed CO_2 molecules, contributing to more orderly adsorption on the surface of the activated carbons.

SYMBOL DESCRIPTION

D – Diffusion coefficient, m^2 · s^{-1}
h – Initial adsorption rate, mL · min^{-1}
K_1 – The quasi-first-order adsorption rate constant, min^{-1}
K_2 – The quasi-second-order adsorption rate constant, mL · g^{-1} · min^{-1}
K_B – Bangham kinetic model constants
K_d – Adsorption thermodynamic equilibrium constant
K_{dif} – Intraparticle diffusion rate constant, mL · g^{-1} · min$^{-1/2}$
K_{fn} – Freundlich isotherm constant
m_t, m_0 – the weights of activated carbon before and after CO_2 adsorption, respectively, g
P – Adsorption equilibrium pressure, Pa
R – Universal Gas Constant, J · mol^{-1} · K^{-1}
R^2 – Fitting correlation coefficient
r – Average radius of activated carbon particles, m
T – Adsorption temperature, K
q_e, $q_{e,cal}$, $q_{e,exp}$, q_t, q_∞ – Respectively, the adsorption amount of CO_2 when the equilibrium is reached, the theoretically calculated adsorption amount of CO_2, the experimentally measured adsorption amount of CO_2, the adsorption amount of CO_2 at any time, and the saturated adsorption amount of CO_2, mL · g^{-1}
q_{est} – Isosteric heat of adsorption, KJ · mol^{-1}
Z – Bangham kinetic model constants
α – Elovich kinetic model initial rate constant, mL · g^{-1} · min^{-1}
β – Elovich kinetic model desorption rate constant, g · mL^{-1}
ΔG – Adsorption Gibbs free energy change, KJ · mol^{-1}
ΔH – The enthalpy change during the adsorption process, KJ · mol^{-1}
ΔS – The entropy change during the adsorption process, J · mol^{-1} · K^{-1}

Subscript

t – Any time of adsorption
0 – Initial time of adsorption

ACKNOWLEDGMENTS

This study was financially supported by Natural Science Foundation of Shandong Province (No.ZR2020QE204) and Doctoral Research Fund of Shandong Jianzhu University (No.X18068Z).

LITERATURE CITED

1. Di Paola, G., A. Rizzo, A.G. Benassai, G. Corrado, F. Matano & P. P. Aucelli (2021). Sea-level rise impact and future scenarios of inundation risk along the coastal plains in Campania (Italy). Environ. *Earth Sci.* 80 (17), 1–22. DOI: 10.1007/s12665-021-09884-0.

2. Aihaiti, A., Jiang, Z., Zhu, L., Li, W. & You Q. (2021). Risk changes of compound temperature and precipitation extremes in China under 1.5°C and 2°C global warming. *Atmospheric Research* 264, 105838. DOI: 10.1016/j.atmosres.2021.105838.

3. Keeling, C.D., Bacastow, R.B., Bainbridge, A.E., Ekdahl Jr, C.A., Guenther, P.R., Waterman, L.S. & Chin, J.F. (1976). Atmospheric carbon dioxide variations at Mauna Loa observatory, Hawaii. Tellus 28 (6), 538–551. DOI: 10.1111/j.2153-3490.1976.tb00701.x.

4. Benson, S., Chandler, W., Edmonds, J., Houghton, J., Levine, M., Bates, L., Chum, H., Dooley, J., Grether, D. & Logan, J.(1998). Assessment of basic research needs for greenhouse gas control technologies, Lawrence Berkeley National Lab., Berkeley, CA (US). ISBN: 9780080430188.

5. Zhang, Y.D. & Zhao, T. (2013). Analysis on emission reduction targets of carbon dioxide in China. Advanced Materials Research, Trans Tech Publ. 734–737, 1891–1895. DOI: 10.4028/www.scientific.net/AMR.734-737.1891.

6. Krishnaiah, D., Bono, A., Anisuzzaman, S., Joseph C., & Khee T.B. (2014). Carbon dioxide removal by adsorption. *J. Appl. Sci*. 14 (23), 3142–3148. DOI: 10.3923/jas.2014.3142.3148.

7. Y Mohd Yazri, M.H. (2013). Development of Ionic Liquid Mixed Matrix Membrane (ILMMM) for Carbon Dioxide Removal. Universiti Teknologi Petronas. http://utpedia.utp.edu.my/id/eprint/8401

8. Abd, A.A., Naji, S.Z., Hashim, A.S. & Othman, M.R. (2020). Carbon dioxide removal through physical adsorption using carbonaceous and non-carbonaceous adsorbents: a re-

view. *J. Environ. Chem. Engin.* 8 (5), 104142. DOI: 10.1016/j.jece.2020.104142.

9. Areán, C.O. & Delgado, M.R. (2010). Variable-temperature FT-IR studies on the thermodynamics of carbon dioxide adsorption on a faujasite-type HY zeolite. *Appl. Surf. Sci*. 256 (17), 5259–5262. DOI: 10.1016/j.apsusc.2009.12.114.

10. Ho, M.T., Allinson G.W. & Wiley, D.E. (2008). Reducing the cost of CO_2 capture from flue gases using pressure swing adsorption. *Ind. & Engin. Chem. Res.* 47 (14), 4883–4890. DOI: 10.1021/ie070831e.

11. Lin, R., Zhuang, L., Xu, X. & Chen, S. (2013). Design of a viscose based solid amine fiber: effect of its chemical structure on adsorption properties for carbon dioxide. *J. Coll. Inter. Sci.* 407, 425–431. DOI: 10.1016/j.jcis.2013.06.029.

12. Horio, M., Suzuki, K., Mori, T., Inukai, K. & Tomura, S., (1997). Method for separation of nitrogen and carbon dioxide by use of ceramic materials as separating agent, Google Patents.

13. Mujmule, R.B., Chung, W.J. & Kim, H. (2020). Chemical fixation of carbon dioxide catalyzed via hydroxyl and carboxyl-rich glucose carbonaceous material as a heterogeneous catalyst. *Chem. Engin. J.* 395, 125164. DOI: 10.1016/j.cej.2020.125164.

14. Hou, M., Qi, W., Li, L., Xu, R., Xue, J. Zhang, Y., Song, C. & Wang, T. (2021). Carbon molecular sieve membrane with tunable microstructure for CO2 separation: Effect of multiscale structures of polyimide precursors. *J. Membr. Sci.* 635: 119541. DOI: 10.1016/j.memsci.2021.119541.

15. Bell, J.G., Benham, M.J. & Thomas, K.M. (2021). Adsorption of Carbon Dioxide, water vapor, nitrogen, and sulfur dioxide on activated carbon for capture from flue gases: competitive adsorption and selectivity aspects. Energy & Fuels 35(9), 8102-8116. DOI: 10.1021/acs.energyfuels.1c00339.

16. Yenisoy-Karakaş, S., Aygün, A., Güneş, M. & Tahtasakal, E. (2004). Physical and chemical characteristics of polymer-based spherical activated carbon and its ability to adsorb organics. *Carbon* 42 (3), 477–484. DOI: 10.1016/j.carbon.2003.11.019.

17. Ma, R., Qin, X., Liu, Z., & Fu, Y. (2019). Adsorption property, kinetic and equilibrium studies of activated carbon fiber prepared from liquefied wood by ZnCl2 activation. *Materials* 12 (9), 1377. DOI: 10.3390/ma12091377.

18. Ramírez, A., Sierra, L., Mesa, M. & Restrepo, J. (2005). Simulation of nitrogen a dsorption–desorption isotherms. Hysteresis as an effect of pore connectivity. *Chem. Engin. Sci.* 60 (17), 4702–4708. DOI: 10.1016/j.ces.2005.03.004.

19. Voigt, W. (1993). Calculation of salt activities in molten salt hydrates applying the modified BET equation, I: Binary systems. Monatshefte für Chemie/Chemical Monthly 124 (8), 839–848. DOI: 10.1007/bf00816406

20. Nunes, C.A. & Guerreiro, M.C. (2011). Estimation of surface area and pore volume of activated carbons by methylene blue and iodine numbers. Química Nova 34, 472–476. DOI: 10.1590/S0100-40422011000300020.

21. Lawrence, N.S. & Wang, J. (2006). Chemical adsorption of phenothiazine dyes onto carbon nanotubes: Toward the low potential detection of NADH. *Electrochem. Commun*. 8 (1), 71–76. DOI: 10.1016/j.elecom.2005.10.026.

22. Rozanov, L. (2021). Kinetic equations of non-localized physical adsorption in vacuum for Freundlich adsorption isotherm. *Vacuum* 189, 110267. DOI: 10.1016/j.vacuum.2021.110267.

23. Azuara, E., Cortes, R., Garcia, H.S. & Beristain, C.I. (1992). Kinetic model for osmotic dehydration and its relationship with Fick's second law. *Inter. J. Food Sci. & Technol.* 27 (4), 409–418. DOI: 10.1111/j.1365-2621.1992.tb01206.x.

24. Crich, D., Jiao, X.Y., Yao, Q. & Harwood, J.S. (1996). Radical Clock Reactions under Pseudo-First-Order Conditions Using Catalytic Quantities of Diphenyl Diselenide. A 77Se- and 119Sn-NMR Study of the Reaction of Tributylstannane and Diphenyl Diselenide. *J. Organic Chem*. 61 (7), 2368–2373. DOI: 10.1021/jo950857s.

25. Ho, Y.S. & Ofomaja, A.E. (2006). Pseudo-second-order model for lead ion sorption from aqueous solutions onto palm kernel fiber. *J. Hazard. Mater*. 129(1–3), 137–142. DOI: 10.1016/j.jhazmat.2005.08.020.

26. Moon, H. & Lee W.K. (1983). Intraparticle diffusion in liquid-phase adsorption of phenols with activated carbon in finite batch adsorber. *J. Coll. Interf. Sci*. 96 (1), 162–171. DOI: 10.1016/0021-9797(83)90018-8.

27. Xiong, F., Hwang, B., Jiang, Z., James, D., Lu, H. & Moortgat, J. (2021). Kinetic emission of shale gas in saline water: Insights from experimental observation of gas shale in canister desorption testing. *Fuel* 300, 121006. DOI: 10.1016/j.fuel.2021.121006.

28. Qin, C., Jiang, Y., Zuo, S., Chen, S., Xiao, S., & Liu, Z. (2021). Investigation of adsorption kinetics of CH_4 and CO_2 on shale exposure to supercritical CO_2. *Energy* 236, 121410. DOI: 10.1016/j.energy.2021.121410.

29. Shen, D., Bülow, M., Siperstein, F., Engelhard, M. & Myers, A.L. (2000). Comparison of experimental techniques for measuring isosteric heat of adsorption. *Adsorption* 6 (4), 275–286. DOI: 10.1023/A: 1026551213604.

30. Fung, V., Hu, G., Ganesh, P. & Sumpter, B.G. (2021). Machine learned features from density of states for accurate adsorption energy prediction. *Nature Commun*. 12 (1), 1–11. DOI: 10.1038/s41467-020-20342-6.

31. Qiu, J., Wang, Y., Wu, P., Jiang, S., Cui, K., Chen, G., Liu, D. & Cui, G. (2021). Adsorption characteristics of hexadecyl ammonium with different numbers of carbon chains in montmorillonite and the structure of the prepared composites. *J. Porous Mat*. 28 (6), 1675–1687. DOI: 10.1007/s10934-021-01114-z.

32. Jin, C., Sun, J., Chen, Y., Guo, Y., Han, D., Wang, R. & Zhao, C. (2021). Sawdust wastes-derived porous carbons for CO_2 adsorption. Part 1. Optimization preparation via orthogonal experiment. Separation and Purification Technology 276, 119270. DOI: 10.1016/j.seppur.2021.119270.

33. Jiao, J., Cao, J., Xia, Y. & Zhao, L. (2016). Improvement of adsorbent materials for CO_2 capture by amine functionalized mesoporous silica with worm-hole framework structure. *Chem. Engin. J.* 306, 9–16. DOI: 10.1016/j.cej.2016.07.041.

34. Jia, J., Wang, Y., Feng, Y., Hu, G., Lin, J., Huang, Y., Zhang, Y., Liu, Z., Tang, C. & Yu, C., (2021). Hierarchically porous boron nitride/HKUST-1 hybrid materials: synthesis, CO_2 adsorption capacity, and CO_2/N_2 and CO_2/CH_4 selectivity. *Ind. & Engin. Chem. Res*. 60 (6), 2463–2471. DOI: 10.1021/acs.iecr.0c05701.

35. Pham, T.H., Lee, B.K. & Kim, J. (2016). Novel improvement of CO_2 adsorption capacity and selectivity by ethylenediamine-modified nano zeolite. *J. Taiwan Inst. Chem. Engin.* 66, 239–248. DOI: 10.1016/j.jtice.2016.06.030.

36. Lee, S.Y. & Park, S.J. (2013). Determination of the optimal pore size for improved CO_2 adsorption in activated carbon fibers. *J. Col. Int. Sci.* 389 (1), 230–235. DOI: 10.1016/j.jcis.2012.09.018.